Participation of off-equatorial wave energy for the Atlantic Niño events identified by wave energy flux in case studies

Qingyang Song[1], Youmin Tang[1] and Hidenori Aiki[2]

1. College of Oceanography, Hohai University, China

2.Institute for Space-Earth Environmental Research, Nagoya University, Japan

Submitted to GRL, Mar., 2023

Introduction

In the tropical Atlantic Ocean, extreme climate events with anomalous sea surface temperature, current, and precipitations are often referred to as the Atlantic Niño.

The Atlantic Niño presents more diversity in its intensity and occurrence time, especially in recent years, e.g. 2019 and 2021. To investigate the mechanism responsible for this diversity, this study focuses on ocean responses to atmospheric forcing, manipulating the wind forcing in both equatorial and off-equatorial regions to excite linear ocean models for three types of events that occurred in 1999, 2019, and 2021 respectively.

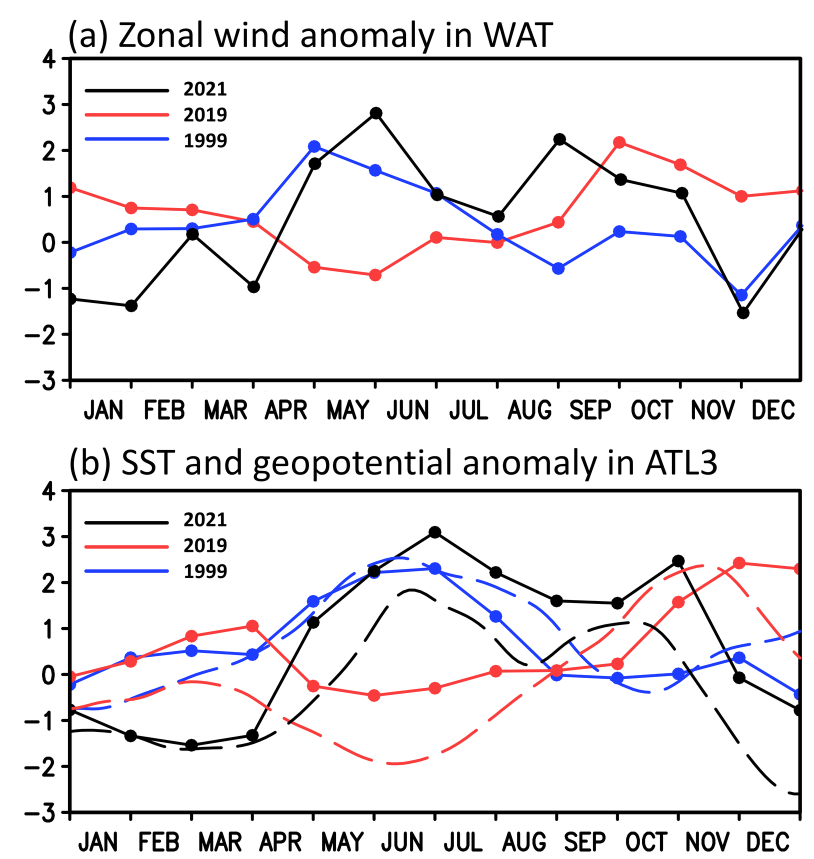

Problems:

1. Can the off-equatorial forcing have a notable influence on the Atlantic Niño?

2. Does the diversity of the Atlantic Niño can owe to wave dynamics?

Figure 1. (a) Timeseries of zonal wind anomaly averaged in the western equatorial Atlantic basin (WAT, 3°S–3°N, 40°W–20°W) in 1999 (blue), 2019 (red) and 2021 (black); (b) Timeseries of SST from OISST (solid line) and geopotential anomaly from the LOM (dashed line) averaged over the Atlantic 3 region (ATL3, 3°S–3°N, 20°W–0°).

Key Points:

1. The spatial sensitivity of wind forcing to three different Atlantic Niño events is investigated with linear ocean models.
2. Wave energy flux by off-equatorial Rossby waves is revealed to excite reflected Kelvin waves during the Atlantic Niño events.
3. The interaction between the wind-forced and the reflected Kelvin waves can lead to the diversity of Atlantic Niño events.

Numerical experiments

Linear ocean model (LOM) :

Model basin	Atlantic Ocean, real coastline
Wind forcing	ERA-5 database
Simulation period	1992-2021
Gravity-reduced model for first four baroclinic normal mode respectively	

$$u'_t - fv' + p'_x = \alpha^{(n)} \frac{\tau^x}{\rho_0\sqrt{h_{mix}H_b}} + \text{SGS}$$
$$v'_t + fu' + p'_y = \alpha^{(n)} \frac{\tau^y}{\rho_0\sqrt{h_{mix}H_b}} + \text{SGS}$$
$$p'_t + (c^{(n)})^2(u'_x + v'_y) = 0$$
$$H^{(n)} = \sqrt{h_{mix}H_b}\,/\alpha^{(n)}$$

Forcing sensitivity experiments in 1999, 2019 and 2021:

T0: apply full zonal wind forcing

T1: apply zonal wind forcing in R1 region

T2: apply zonal wind forcing in R2 region

T3: apply zonal wind forcing in R2 region

T4: remove all zonal forcing.

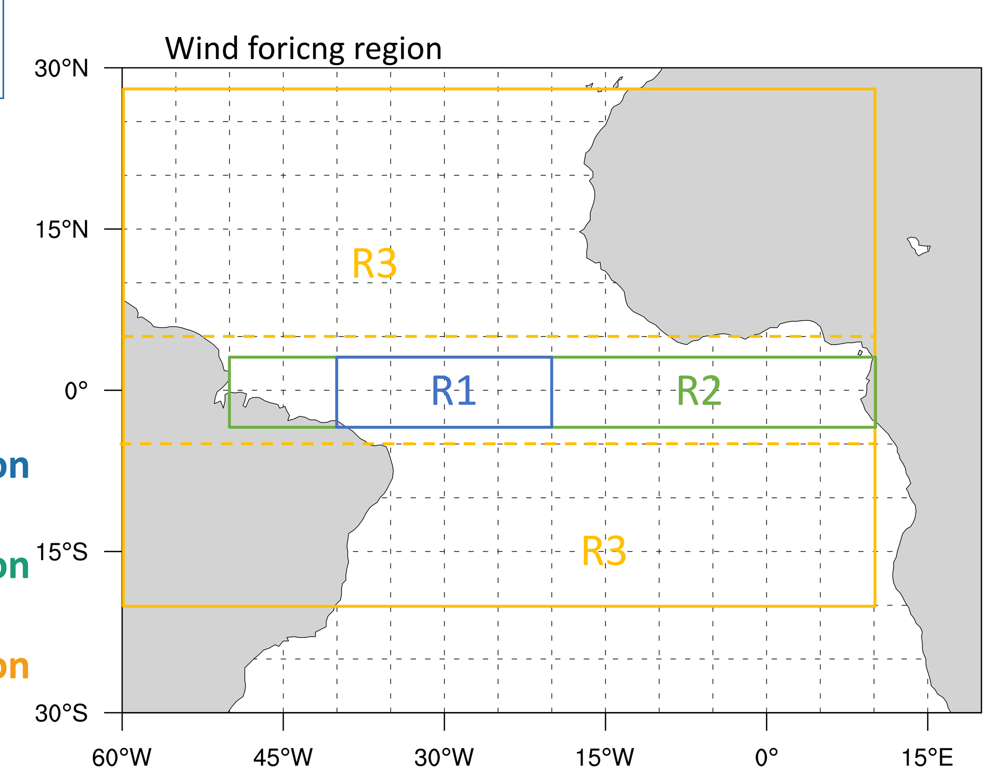

Figure 2. Three forcing region marked by R1 (WAT), R2 3°S–3°N, 60°W–10°E) and R3 (20°S–3°S, 3°N–28°N, 60°W–10°E).

Simulation results

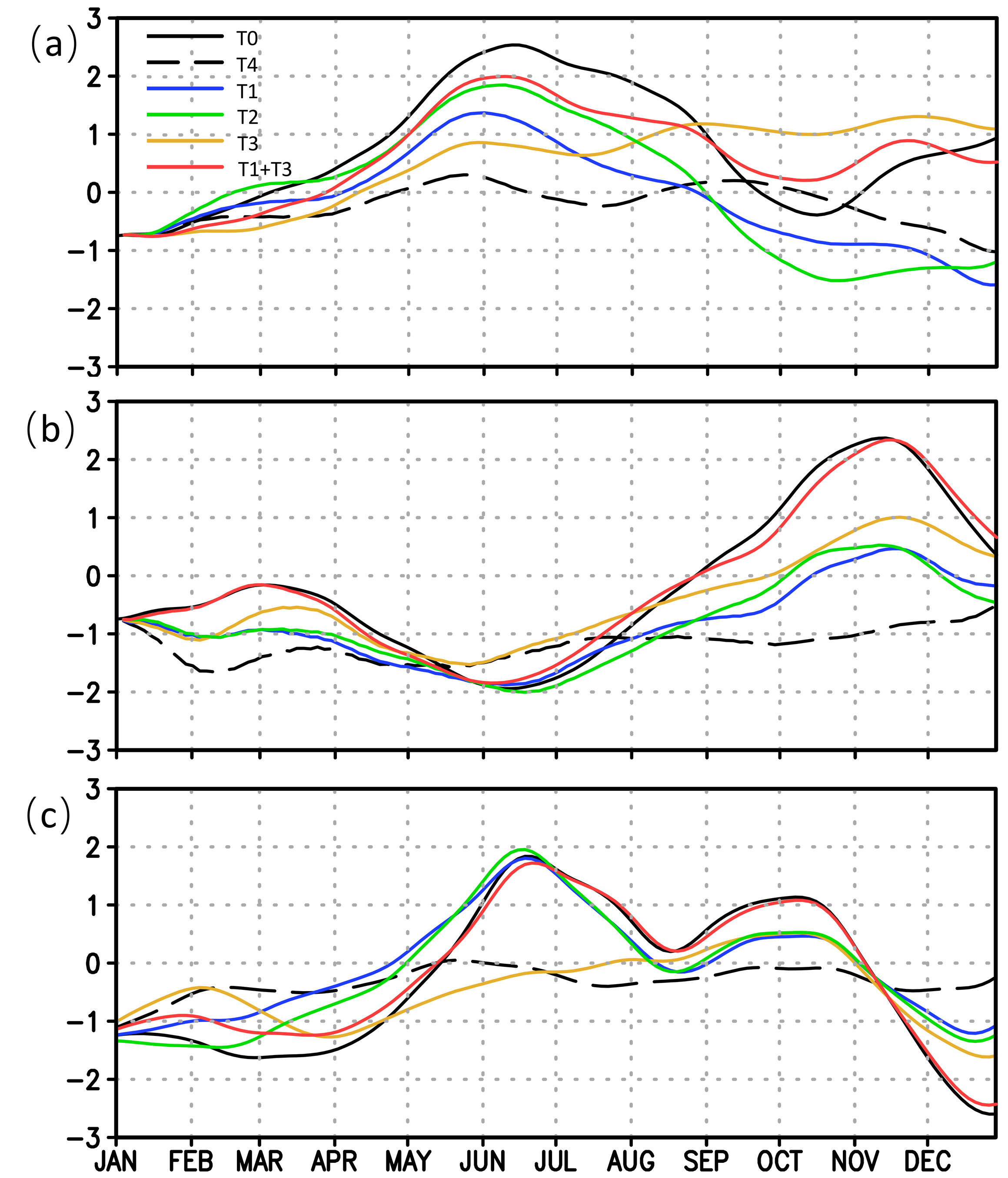

Figure 2. Timeseries of averaged geopotential anomaly in ATL3 from the sensitivity experiments in (a)1999, (b)2019 and (c)2021. The geopotential anomaly is obtained after being normalized by the variance of the reference run in the period from 1992 to 2021.

Wave energy flux at the equator

AGC-L2 flux:

$$\vec{c_g}\overline{E} \approx \overline{\vec{V}^{(n)}p^{(n)}} + \nabla \times (\overline{p^{(n)}(\varphi^{(n)})}/2)\vec{z}$$

φ:

$$\Delta\varphi^{(n)} - (f/c^{(n)})^2\varphi^{(n)} = q^{(n)}$$

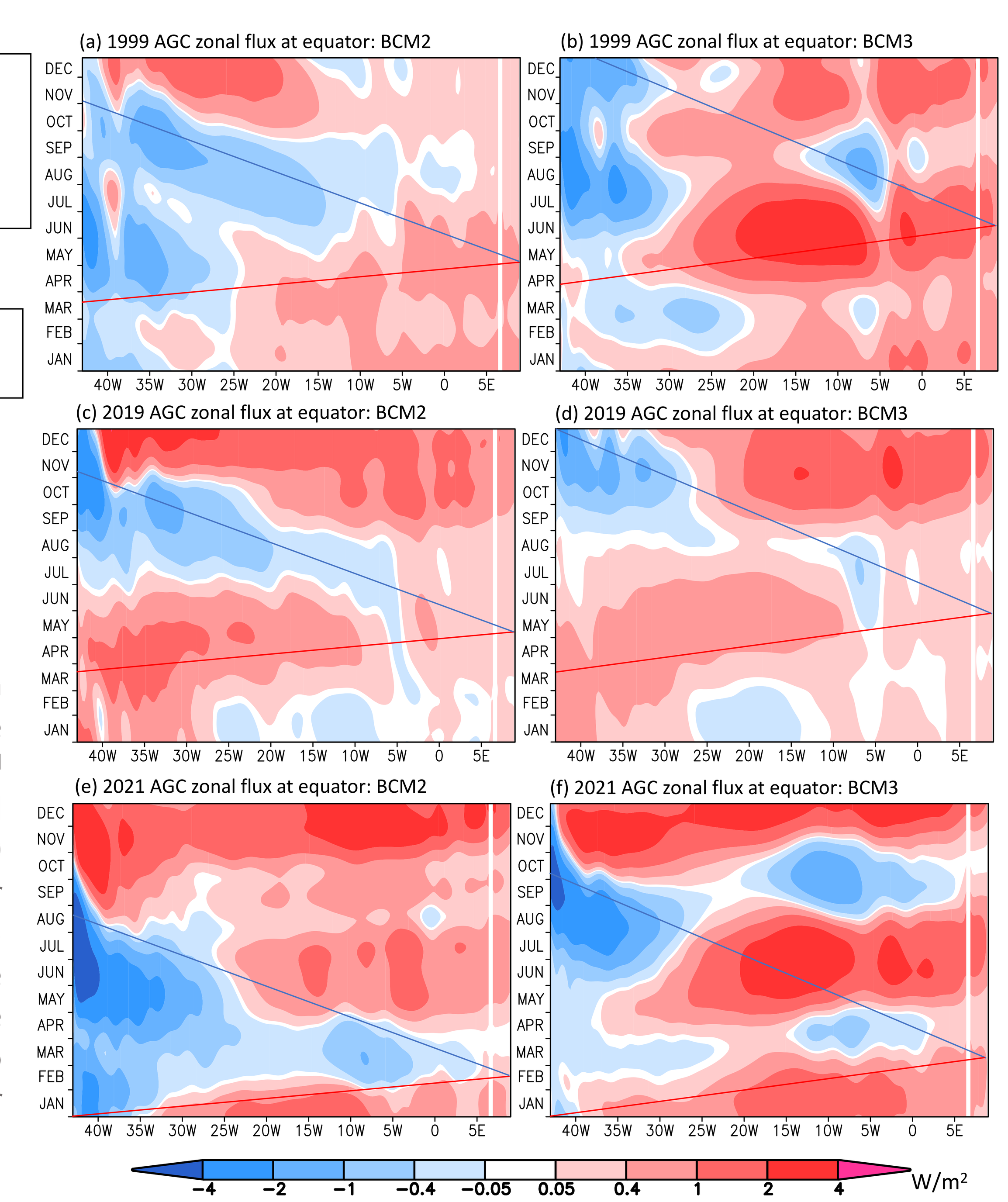

Figure 3. Hovmöller diagram for the AGC-L2 flux at the equator in the 2nd and 3rd baroclinic mode (BCM2 and BCM3) in 1999 (a,b), 2019 (c,d), and 2021 (e,f). Color shadings are the zonal AGC-L2 flux at the equator; The solid red (blue) line represents theoretical group velocity of the KW (RW) for the corresponding BCM.

Energy streamfunction and potential by off-equatorial forcing

$$-\frac{\partial S}{\partial y} - \frac{\partial P}{\partial x} = \rho_0\overline{u^{(n)}p^{(n)}} + \rho_0\frac{\partial}{\partial y}(\overline{p^{(n)}\varphi^{(n)}}/2)$$
$$+\frac{\partial S}{\partial x} - \frac{\partial P}{\partial y} = \rho_0\overline{v^{(n)}p^{(n)}} + \rho_0\frac{\partial}{\partial x}(\overline{p^{(n)}\varphi^{(n)}}/2)$$

S: stream function
P: potential

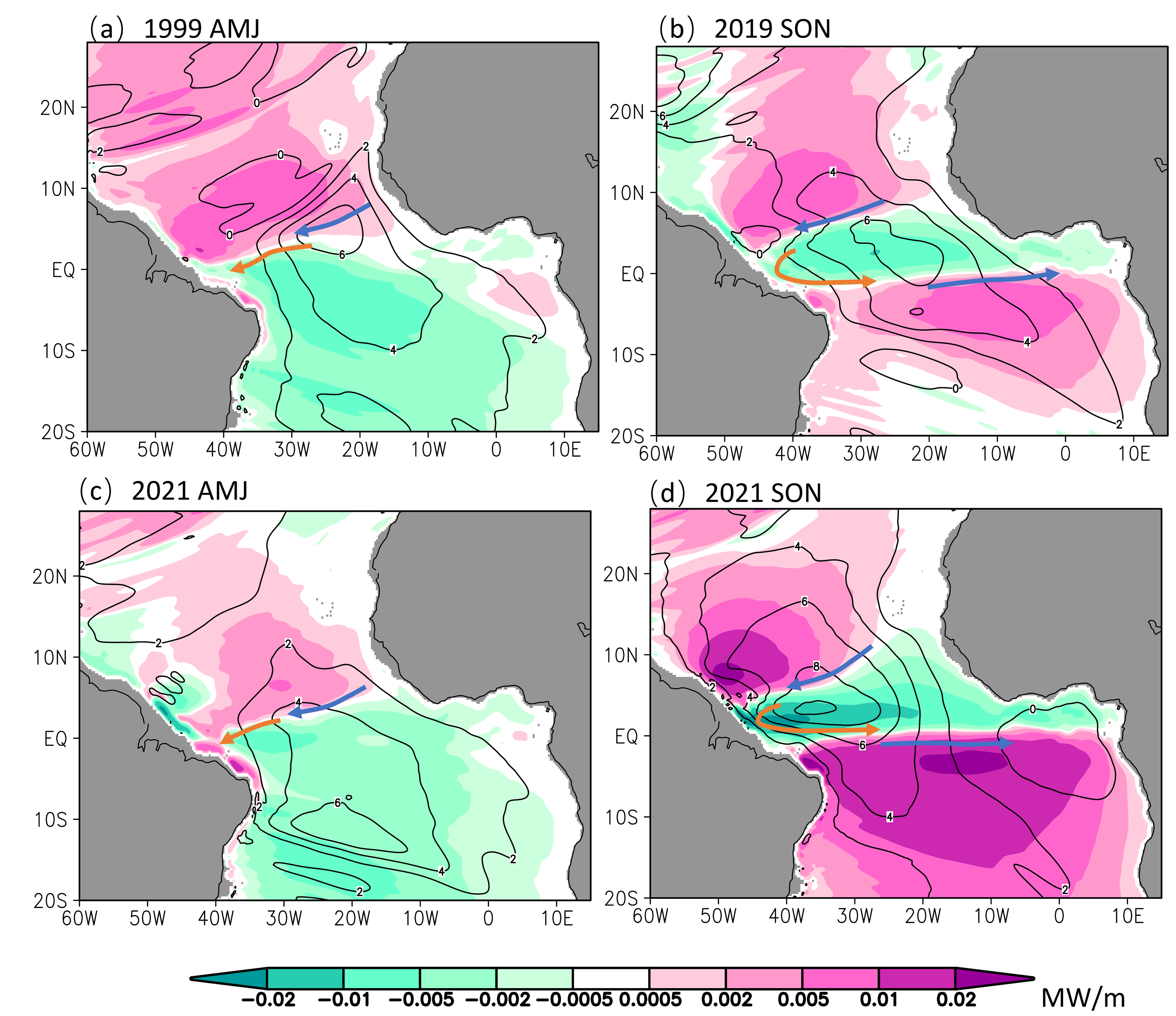

Figure 4. The mean streamfunction and potential for the AGC-L2 flux over AMJ (April to June, left panel) and SON (September to December) in the four events for T2 off-equatorial forcing scenarios in the 2nd baroclinic mode. Color shading: streamfunction *S*. Contour: potential *P* for the AGC-L2 flux with an interval of 2 KW/m. The blue (orange) arrow line indicates the direction of the clockwise (anti-clockwise) streamline.

Conclusions

1. The sensitivity experiments suggest that the off-equatorial zonal wind is capable of affecting equatorial waves in the Atlantic basin by inducing negative thermocline displacement so as to trigger the Atlantic Niños in 2019 and 2021 winter.

2. Independent waveguide are identified by wave energy flux to reveal the dual wave energy sources for the equatorial Kelvin waves (KWs): one is the local wind forcing in the western tropical basin; the other is the reflection due to the off-equatorial Rossby waves in the western boundary.

3. The reflected KWs can precondition the events when wind-forced KWs insufficiently displace the thermocline (e.g. the boreal winter of 2019 and 2021). Background waves with positive geopotential anomaly contribute to triggering the Niño events and vice versa. The participation of off-equatorial wave energy hence leads to the diversity of the Atlantic Niños.